TRENDS IN SCIENCES 2026; 23(7): 13233
https://doi.org/10.48048/tis.2026.13233 REVIEW ARTICLE

Low-Cost Silica Aerogels from Waste-Derived Ashes via Atmospheric Pressure Drying: A Systematic Review of Synthesis Strategies, Properties, and Application

Iwan Rusiardy[1,2,*], Muhammad Romli [3], Erliza Noor [3], Suprihatin Suprihatin[3] and Sukma Surya Kusumah[4]

[1]Doctoral Student of Agroindustry Engineering and Technology, Faculty of Engineering and Technology, IPB university, Kampus IPB Dramaga, Bogor 16680, Indonesia
[2]Department of Agricultural Technology, Pontianak State Polytechnic, Pontianak 78124, Indonesia
[3] Division of Agroindustry Engineering and Technology, Faculty of Engineering and Technology, IPB university, Kampus IPB Dramaga, Bogor 16680, Indonesia
[4]Indonesian National Research and Innovation Agency (BRIN), Research Center for Biomass and Bioproducts, Bogor 16915, Indonesia

([*]Corresponding author's e-mail: iwanrusiardy28@gmail.com)

Received: 31 December 2025, Revised: 14 February 2026, Accepted: 21 February 2026, Published: 10 March 2026

Abstract

Silica aerogel (SA) is a very light porous material that has been widely explored for applications in thermal insulation, adsorption, catalysis, and environmental remediation, even in the health sector. SA in this review is made from waste-based ashes, which include coal fly ash and biomass ash. Silk aerogel from waste ash has been widely studied at the laboratory scale, but until now, it has not been adapted to the industrial scale due to the high processing costs and the complexity of the drying method used. In this case, atmospheric pressure drying (APD) is a possible alternative method for producing SA at a low cost and easier so that it can be applied on an industrial scale. This study presents a systematic literature review on the synthesis of silica aerogel from waste-based ashes with a special emphasis on the APD-based process along with a concise application carried out following the PRISMA 2020 guidelines, including the stages of identification, screening, and assessment of the eligibiliexpenses reputable journal articles. The discussion focuses on the silica extraction pathway through initial pretreatment, calcination, sol-gel process conditions, aging process, solvent exchange, surface modification strategies required to maintain the porous structure during drying at atmospheric pressure, and a brief discussion of the application of silica aerogels from waste-based ash. The results of the literature synthesis indicate that the character of the ash source determines the need for pretreatment, the pH of the sol-gel plays a crucial role in maintaining the stability of the hydrolysis-condensation reaction, the aging process is essential in establishing structural stability, and surface modification through silylation is crucial to prevent pore collapse and excessive shrinkage during APD. Optimization of the alkali fusion ratio and reaction conditions affects the efficiency of silica extraction, and last but not least, time and temperature are crucial in achieving the best SA. This review identifies challenges related to the evolution of pore structure during APD and highlights the need to develop sustainable and scalable APD protocols for industrial applications.

Keywords: Silica aerogel, Sol-gel process, Waste-derived ashes, Atmospheric pressure drying, Structure-property relationship, Low-cost synthesis, Systematic literature review

Introduction

Silica aerogel is one of the most promising thermal insulation materials [1]. Over the past decade, although not as extensive as research on SA from synthetic precursors, such as TEOS and TMOS, interest in waste-derived ashes-based aerogels has steadily increased due to environmental concerns, high synthesis costs, and the toxicity of synthetic precursors, despite producing high-quality aerogels [2]. As a solution, the use of coal and biomass combustion ash has begun to be widely explored as a more sustainable alternative silica source within a circular economy framework [3,4]. Waste-derived ash production, particularly fly ash (FA), a byproduct of coal and biomass combustion, continues to increase along with the expansion of the worldwide energy and manufacturing industries. Furthermore, the increasing use of biomass as a renewable energy source has also contributed to the accumulation of significant amounts of biomass ash [5]. The accumulation of waste-derived ashes without proper management will pose environmental problems [6,7].

Numerous review articles have addressed SA from the perspectives of synthesis, physical properties, and applications. However, most of these studies are reported in a fragmented manner, emphasizing specific steps, such as silica extraction or surface modification, without a conceptual synthesis linking the stages comprehensively. Consequently, the causal relationship between raw material variability and final SA performance remains unsystematized in the reviewed literature, even though this aspect is crucial for the successful transition from laboratory scale to industrial applications. Therefore, SA synthesis using a natural silica waste-based approach is increasingly being viewed as a more environmentally friendly synthetic route with potential for industrial-scale development. However, a coherent cross-stage framework that systematically connects precursor variability to APD performance remains lacking. This work proposes an integrated, mechanism-based framework linking ash precursor variability to sol-gel kinetics, pore evolution, and shrinkage control during atmospheric pressure drying (APD). Focusing on coal and biomass-derived ashes and APD-based routes, this review provides a cross-stage roadmap to support process optimization and scalability-oriented decision-making.

Silica aerogel from waste-derived ashes has a very low density (0.08 - 0.19 g/cm^3), high porosity (> 80%), very low thermal conductivity (0.042 - 0.050 W/mK), a very high specific surface area of 481 - 810 m^2/g, high pore volume (0.991 - 5.19 cm^3/g), mesopore diameter (2.24 - 18.86 nm), and a contact angle of up to 140° [8-15]. Based on its extraordinary properties, waste-derived ash-based SA can be applied in various fields that require high thermal insulation and adsorption properties. Such as, in the field of construction materials such as mortar, cement, and gypsum construction materials [16-18]. In the environmental field, SA has a high ability to reduce CO_2 [9], as well as to remove heavy metals such as Pb^{2+}, Cd^{2+}, Cu^{2+}, and U(VI) [19,20], along with dyes [14]. SA can serve as supports for photocatalytic processes, enhanced efficacy in the degradation of organic compounds [15,16]. And in the health sector, SA has potential as a drug delivery system [17,21].

Although various applications show great potential in industrial waste reduction and sustainable materials development, the transition of this technology to commercialization still faces substantial scientific and technical barriers. Based on our analysis, several systemic challenges in the current literature need to be highlighted: Production Efficiency Constraints: Traditional sol-gel processes, which culminate in Ambient Pressure Drying (APD), are still dominated by time-consuming procedures, particularly during the gel network maturation and solvent diffusion stages. This creates a significant economic barrier to mass production, where optimization of process kinetics is often neglected in favor of laboratory-grade quality.

Structural Integrity in Composite Applications: Efforts to incorporate aerogels into large-scale construction matrices often face issues of brittleness and interfacial instability. A lack of understanding of the molecular interactions between aerogel particles and gypsum materials leads to degradation of mechanical performance, hindering their practical use as standard insulation panels. Long-Term Performance Uncertainty: Most current studies are limited to short-term performance testing under ideal conditions. There is still little literature exploring how these waste-based SA nanoporous structures withstand exposure to complex pollutants or extreme environmental fluctuations over

long periods of time, which are actually key indicators of the success of a sustainable material.

Adhering to the PRISMA 2020 framework, this review delivers a systematic assessment of recent breakthroughs in SA synthesis using waste-derived precursors. We specifically scrutinize the efficiency of various silica extraction pathways, the gradations of sol-gel kinetics, and the critical role of surface modification in confirming successful Atmospheric Pressure Drying (APD). By synthesizing these technical facets, this work aims to establish a cohesive roadmap for transitioning waste-based aerogels from small-scale laboratory experiments toward viable, safe, and sustainable industrial-scale production.

In summary, this review consolidates dispersed evidence into actionable process-parameter recommendations for preserving nanoporous microstructure and minimizing shrinkage under APD, thereby supporting scalability-oriented development of ash-derived silica aerogels**.**

Methodology

This systematic literature review (SLR) adhered to the Preferred Reporting Items for Systematic Reviews and Meta-Analyses (PRISMA) outline. The study investigates literature regarding silica aerogels (SA) produced from fly ash and biomass ash, specifically looking at their synthesis, characterization, and applications of silica aerogel. A thorough literature search was carried out using major databases such as Scopus, Google Scholar, and CrossRef.

This search targeted peer-reviewed journal articles and conference proceedings published in various international journals and academic platforms from 2010 to 2025. This shows a significant increase in publications on waste-based silica aerogels, as well as the development of the atmospheric pressure drying (APD) approach as a more potential alternative for large scale applications. The entire process relied on the main keywords: “silica aerogel” AND “ash”. These core keywords were selected for search sensitivity, while technical relevance (e.g. fly ash/biomass ash, sol-gel, surface modification, and PPE) was confirmed at the screening stage.

The initial search strategy yielded a total of 65 documents limited only to peer-reviewed journals and conference papers. All identified articles underwent a systematic screening process, starting with the elimination of duplicates and followed by a manual evaluation of the titles and abstracts. Through this through manual screening, irrelevant papers were filtered out, resulting in a final selection of 65 eligible articles that strictly aligned with the research scope. These articles were chosen based on specific inclusion criteria, focusing on waste-derived ash-based SA synthesis using sol-gel methods, surface modification, and Atmospheric Pressure Drying (APD). The sol-gel route leading to APD was chosen because APD is an approach that meets the needs of large-scale production at low cost, making it relevant for the purpose of the study highlighting aspects of the laboratory-industry transition.

Studies lacking adequate methodological or experimental detail were excluded, particularly when key process parameters were not reported, as this prevents meaningful cross-study comparison and mechanistic interpretation. Data extraction from the final dataset focused on publication year, precursor type, synthesis parameters, and application domains. These extraction variables were selected because they are the most consistently reported and directly relevant for mapping process-structure-property relationships.

To enhance reliability, only studies reporting quantitative textural parameters such, as BET surface area, pore volume, density, and contact angle were included in cross-study comparisons. Inclusion-exclusion criteria were documented, and reasons for exclusion were recorded during full-text assessment. The robustness of the synthesis was strengthened through structured data extraction and cross-checking of key parameters (silica extraction conditions, pH/acidification, aging, solvent exchange, surface modification, and APD conditions).

Study heterogeneity (precursor ash types, processing conditions, and characterization metrics) was explicitly considered, and conclusions were derived from recurring cross-study patterns rather than isolated findings. It should be noted that reported values vary due to differences in precursor composition, extraction conditions, silicate modulus, and drying protocols. Therefore, absolute numerical comparisons should be interpreted with caution, and emphasis is placed on mechanistic consistency rather than isolated

performance values. **Figure 1** shows the article selection procedure, as depicted in the PRISMA flowchart.

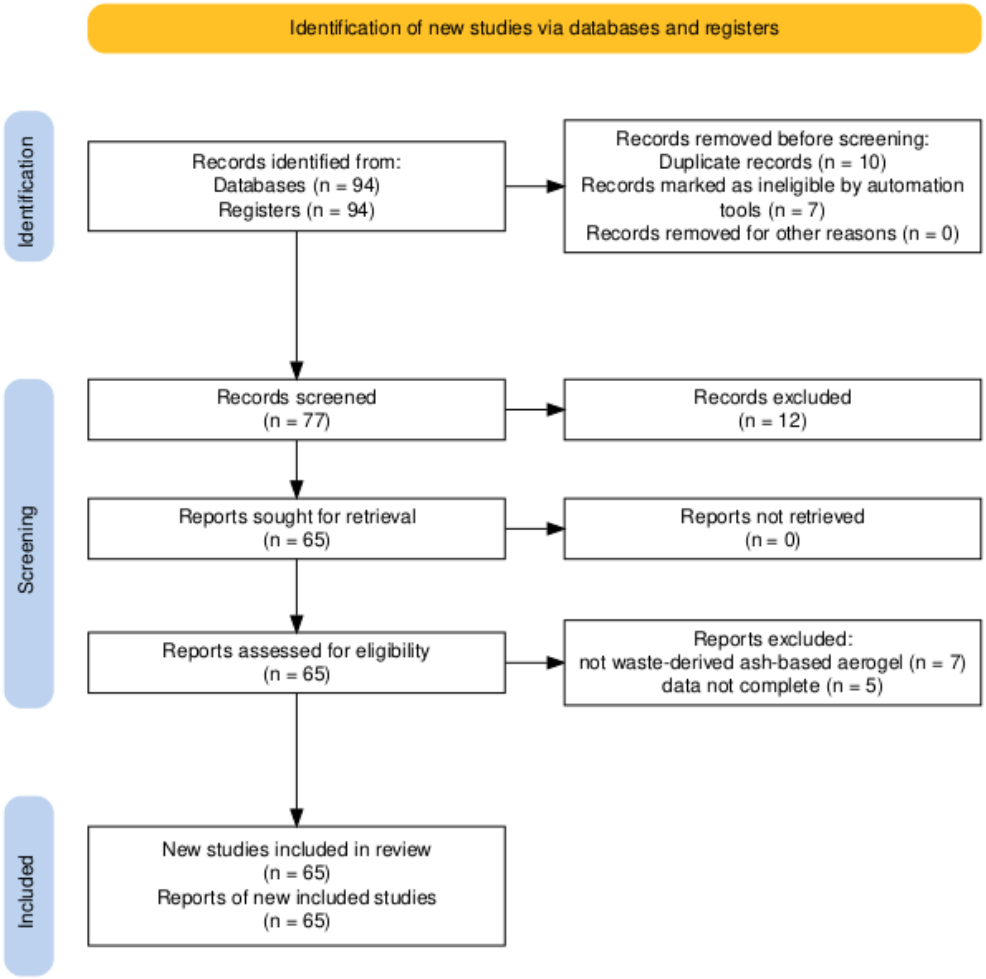

Figure 1 PRISMA 2020 flow diagram illustrating the systematic literature selection process for waste-derived ash silica aerogel synthesis via APD.

Results and discussion

Pretreatment

Raw material characterization and initial pretreatment

The initial pretreatment stage is a critical phase in the synthesis of waste ash-based silica aerogels. The purpose is to standardize chemical and physical processes to mitigate the inherent variability of raw materials. This stage generally includes grinding, sieving, and washing to increase the purity of silica while preparing the particle morphology to be more reactive in the alkali fusion and acid leaching stages. The milled waste ash is then sieved (100 - 200 mesh) to reduce it to 0.15 - 0.074 mm with a uniform particle distribution. This precise size control is expected to provide more controlled reaction conditions and improve reaction consistency [22,23].

In the absence of stringent particle size control, managing reaction conditions becomes challenging, which may lead to the formation of inhomogeneous sols and jeopardize the integrity of the gel network during maturation [24,25]. Particle size affects the specific surface area and reaction rate. In Başgöz's study [19], reducing the ash particle size to the nanoscale was reported to increase the surface area and accelerate the reaction during sodium silicate formation. Therefore, without good particle size control, the dissolution process can be non-uniform and potentially produce less homogeneous sols.

Washing aims to eliminate impurities that may inhibit or interfere with the consistency of the

subsequent reaction [26]. This process can decrease inorganic salts, heavy metal ions, and other interfering components such as Na, Cr, Ni, Cu, Ga, Ba, Pb, and S. Consequently, washing has been reported to increase the purity of silica up to 95.56% and significantly reduce other oxide fractions such as CaO, MgO, P_2O_5, SO_3, K_2O, Al_2O_3, Fe_2O_3, and MnO [25]. Although most studies do not explicitly include the washing process, analysis of FA composition from various sources (**Table 1**) reveals significant variations in the contents of Al_2O_3, CaO, MgO, and Fe_2O_3. This pattern underlines that initial pretreatment is a crucial step for reducing impurities and increasing silica content, especially for FA.

The removal of these interfering ions results in the formation of a stable aerogel network, improves sol homogeneity, and prevents premature condensation and structural collapse during drying. Metal ions, if not removed, may function as catalysts that promote premature precipitation prior to the complete formation of the silica network [27]. Furthermore, washing helps preserve the spherical nanoparticle morphology, which facilitates interparticle necking and the formation of a continuous 3-dimensional porous skeleton during the sol-gel process [25,28]. Ultimately, this initial pretreatment confirms that the resulting silica precursor has sufficient purity and chemical stability, supporting the production of silica aerogels with a uniform pore structure.

Table 1 Chemical composition of coal combustion fly ash (%) and biomass ash based on a literature review (2010 - 2025).

Component	Fly Ash (Coal) (%, w/w)	Biomass Ash (RHA) (%, w/w)
Silica (SiO_2)	47.5 - 66.3 (Avg: 55.0)	85.14 - 92.07 (Avg: 88.6)
Alumina (Al_2O_3)	13.0 - 33.5 (Avg: 24.7)	0.4
Iron Oxide (Fe_2O_3)	4.1 - 11.6 (Avg: 7.8)	0.24
Other Oxides (CaO, MgO, dsb)	1.34 - 23.0 (Avg: 9.8)	0.24 - 5.02 (Avg: 1.9)
Total Major Oxides (SiO_2 + Al_2O_3 + Fe_2O_3)	> 75% (Avg: 87.5)	> 85% (Avg: 89.2)
Loss on Ignition (LOI) / Carbon	-	1.53

Note: Data are summarized from selected studies [8,22,24,26,34,37,54].

Thermal pre-treatment: Calcination

Calcination plays a major role in increasing the reactivity of the aluminosilicate phase through the cleavage of Si–O–Si and Si–O–Al bonds in both amorphous and crystalline components, including mullite, vitreous phase, ferrite, and amorphous carbon [8,27]. By reducing network polymerization and creating defect sites, the disrupted framework becomes more reactive and more easily converted into soluble silicate species [28]. Thermal activation at elevated temperatures promotes the formation of soluble silicate species by disrupting the structural regularity of aluminosilicates. This aligns with the findings of Criado *et al.* [29] who stated that amorphous aluminosilicate content is a prerequisite for producing highly reactive materials through the activation process. Furthermore, several study reports state that calcination activation combined with alkalis such as sodium carbonate (Na_2CO_3) and sodium hydroxide (NaOH) significantly increases the formation of reactive phases. Under these conditions, the reaction of SiO_2 and Al_2O_3 with Na_2CO_3 forms compounds such as Na_2CO_3. $AlSiO_4$, which are readily soluble in acidic solutions, thereby increasing the efficiency of the desiccation process [22,23].

The porosity of SA increases with increasing firing temperature during preparation until it reaches optimum conditions [23]. Calcination at an optimal temperature of 900 °C with sodium carbonate for 3 hours produces the highest degradation rate, forming the readily soluble compound Na_2CO_3. $AlSiO_4$ [30]. Equally, Wu *et al.* [26] reported that the optimal calcination temperature is 850 °C with a holding time of 2 h, accelerating the formation of $NaAlSiO_4$ and Na_2SiO_3.

The data also indicates that temperatures below 750 °C are insufficient to optimally lyse the silicate phase. At this temperature, fly ash activation is not optimal because the crystalline quartz and especially mullite phases are still stable and difficult to decompose/transform at this temperature. As a result, the quartz–mullite peak is still detected in the XRD, indicating that the aluminosilicate network is not yet "open" enough to form a reactive phase. More pronounced transformation only occurs at higher temperatures, so 750 °C is considered insufficient for silicate phase activation [26]. However, calcination performed at 1,000 °C successfully formed an SA with a surface area of 241 m^2/g, showing the formation of silica nanostalactite structures within the cristobalite phase [19].

Alongside temperature factors, the mass ratio of waste ash to alkali is essential. Wu *et al.* [26] indicated that the ideal ratio of FA to alkali trona ore is 1:0.6 (s/s), which was most effective in breaking the aluminosilicate structure. Sun *et al.* [27] stated the optimal ratio of FA to NaOH was 1:1.2 at 550 °C for 2 h, reaching Si and Al leaching efficiencies of 96.92% and 91.36%, respectively. Experimental observations suggest that the use of excess alkali increases CO_2 release but remains effective only up to the optimum saturation point [23,26,27]. High ratios lead to significant structural damage, resulting in unreactive byproducts, while excessively low ratios lead to inadequate activation.

The inclusion of alkalis serves as a dual activation strategy that enhances the cleavage of Si–O and Al–O bonds, turning unreactive ash into soluble sodium silicate and sodium aluminosilicate compounds [26,28]. According to Criado *et al.* [29], this alkaline activation process triggers the dissolution of silicon and aluminum species, which subsequently facilitate the formation of new polymerization structures. This conversion process eliminates structural barriers that impede gelation. However, excessive temperatures may lead to the formation of insoluble silicate phases, such as $NaAlSi_2O_6$, which diminishes the purity of dissolved silica and disrupts the pore network [26]. Therefore, calcination necessitates a careful equilibrium between kinetics and thermodynamics. The success of this stage is fundamentally connected to the initial pretreatment; the reduction of interfering ions and the increase in reactive surface area from washing and grinding enhance the reactivity of FA during alkali fusion. Xia *et al.* [28] noted that impurity ions are commonly removed prior to gelation and demonstrated impurity removal via repeated water washing and solvent exchange (including Fe^{3+} removal). Such purification helps stabilize the precursor chemistry, while the development of an extensive reactive/porous surface is reflected by the high specific surface area reported under optimized conditions. Systematic investigation of these interconnected variables is required to optimize silica conversion efficiency while minimizing total energy consumption.

Figure 2 illustrates the preparation process of fly ash and biomass ash, encompassing key steps such as calcination, alkaline dissolution, and filtration. The resulting process yields a silica solution that serves as a precursor for subsequent synthesis stages.

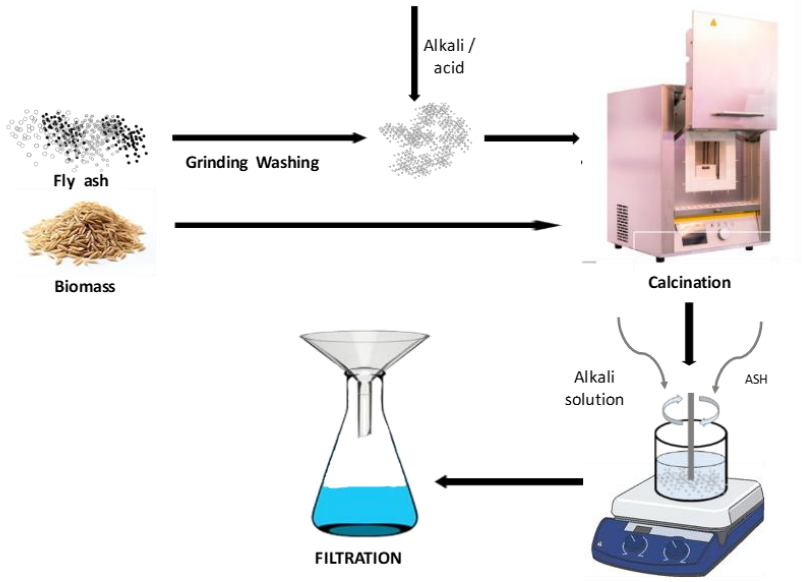

Figure 2 Schematic diagram of preparation of the fly ash and biomass ash.

Alkali hydrolysis

Alkali leaching and silica sol recovery

Alkaline hydrolysis plays a critical role in enhancing the quality of dissolved silica by effectively reducing inorganic mineral contaminants and dissolving amorphous silica from waste ash into soluble sodium silicate, commonly known as water glass. The improvement in the 'quality' of dissolved silica during alkaline hydrolysis primarily refers to an increase in the fraction of Si that is actually dissolved as the more reactive sodium silicate (water glass) species for gelation. This occurs because NaOH weakens/decomposes the Si–O–Si and Si–O–Al networks in the amorphous/aluminosilicate phase, resulting in more efficient silica dissolution and a more homogeneous precursor solution [23,28].

Beyond extraction, this mechanism enhances the reactivity of precursors during the subsequent gelation phase [25]. The efficiency of this process is significantly influenced by the mass ratio of alkali to ash, reaction temperature, duration, and NaOH concentration. According to Qin *et al.* [8], the kinetics of silica dissolution reach their maximum at a 3-hour reaction time, using a 15% NaOH concentration and an alkali-to-ash ratio of 0.4, yielding a dissolution rate of 17.56%. In contrast, Lei *et al.* [31] demonstrated a significantly higher extraction efficiency, achieving a 42% increase in silica recovery by applying 20 wt% NaOH at 100 °C. These variations emphasize that results are frequently dictated by the specific reactivity and mineralogical composition of the waste ash utilized.

The interaction between sodium hydroxide and amorphous silica dominates the initial reaction phase, resulting in the formation of a liquid phase containing soluble sodium silicate. In alkaline media (pH > 10), silica exhibits high solubility and is converted to Na_2SiO_3, and NaOH is reported to preferentially solubilize amorphous silica relative to more ordered silica phases [32]. However, as the reaction time extends, the dissolution of aluminum oxide becomes an important factor. Aluminum interacts with sodium hydroxide to form an insoluble byproduct, sodium aluminosilicate. This precipitate covers the unreacted silica surface and consumes the available alkali, which explains the observed plateau or decline in the dissolution rate after the optimal 3-hour duration [8,33]. While increasing NaOH concentrations can lead to greater mixture uniformity and higher sodium silicate yields, excessive alkali volumes may ultimately decrease the modulus value of the resulting solution [33].

The specific surface area and pore properties of the resultant SA are primarily governed by the modulus of the sodium silicate, specifically the mole ratio of silica to Na_2O [34,35]. Research indicates that at a low modulus of 1.45, the sol fails to gel because the excessive alkalinity hinders the establishment of a stable cross-linked network and obstructs silica

polymerization. Conversely, by increasing the modulus to 4.26, the structural properties of SA are significantly enhanced, yielding an ultra-low density of 0.071 g/cm³, a maximum pore volume of 0.899 cm³/g, and a high specific surface area of 945.8 m²/g [33]. Optimal extraction conditions were further identified by Cui *et al.* [36] at a molar ratio of n(SiO_2):n(NaOH) of 5:4, which serves as an effective precursor for SA synthesis with a silica dissolution rate exceeding 90%. While alternative alkali systems, such as NaOH/$NaHCO_3$ at low temperatures, offer pathways for increasing silica content, their efficiency remains below conventional high-temperature NaOH methods [8]. The lower performance of NaOH/$NaHCO_3$ at low temperatures is mainly attributed to its limited alkalinity, which reduces the effective OH^- activity required to depolymerize aluminosilicate networks into soluble silicate species [28]. This emphasizes the necessity of balancing extraction efficiency with compositional stability to ensure successful integration into the subsequent aerogel synthesis stages.

Sol-gel initiation and acid purification

Based on the literature (**Table 3**), most studies on the synthesis of silica aerogels based on sol-gel APD reported that the sol-gel initiation stage was carried out under acidic conditions. This condition is in line with the silica purification stage after alkali extraction and allows the formation of hydrated silicic acid as a gel precursor through the addition of strong mineral acids such as hydrochloric acid (HCl) and sulfuric acid (H_2SO_4), and in some cases weak organic acids such as acetic acid and oxalic acid. Only a small number of studies reported the application of basic or neutral-basic conditions during the gelation stage, which is generally carried out by adding aqueous ammonia (NH_4OH) to adjust the pH of the silicate solution to the range of pH 5 - 6 [11] or pH around 3.0 [14] which is then increased to a limited extent to neutral conditions before the aging process. Notably, this acid-driven gel initiation is preceded by alkaline extraction in which NaOH preferentially solubilizes the amorphous silica fraction to form reactive sodium silicate (water glass), whereas crystalline phases such as quartz are comparatively more refractory and dissolve more slowly under comparable alkaline conditions [32].

After the alkali hydrolysis process is completed, the resulting sodium silicate solution is generally continued to the acid leaching stage. Acidification simultaneously removes co-dissolved metal ions and shifts soluble silicate toward silicic acid, thereby initiating controlled gelation and Si–O–Si network formation. This stage plays an important role in removing metal contaminants such as Fe, Al, Ti, and Ca, thus obtaining high-purity silica precursors. This purification is considered crucial to support the formation of a stable gel network as well as the development of an adequate porous structure. Various studies have reported that strong mineral acids are most often used at this stage, as they are able to dissolve metal impurities as soluble salts while silica precipitates in the form of hydrated silicic acid (H_2SiO_3) [37].

The type of acid selected plays a central role in determining the character of SA [38]. The application of strong mineral acids (HCl, HNO_3, H_2SO_4) and organic acids (acetic acid, oxalic acid) leads to comparable pore sizes; however, the choice of acid type influences the surface texture of SA. While oxalic acid yields a specific surface area of 322.5 m²/g, hydrochloric acid results in 268 m²/g. This observation suggests that the specific type of acid is more influential in shaping surface morphology than the dimensions of the pores themselves [38].

The efficacy of this process is significantly influenced by the concentration of acid and the operating temperature. Zhang *et al.* [23] specify that the optimal circumstances for reaching determined leaching rates include the application 20% of HCl at 100 °C. Additionally, the pH of the sol solution plays a crucial role in governing the gelation mechanism. Adjusting the sol pH to a range of 2.7 and 3.1 has been documented to produce SiO_2–Al_2O_3 aerogels with a surface area reaching as high as 897 m²/g. Nonetheless, when the pH is reduced below 2.7, the gel structure often becomes excessively dense, leading to a reduction in its surface area. This proposes that a pH level near 3 serves as the equilibrium point for increasing the solubility of impurities while conserving the small size of silica particles, thereby facilitating enhanced ion diffusion [20].

Alongside chemical factors, the physical ratio of the acid volume to the weight of calcined ash (v/m) and the silica-to-water ratio (SiO_2/H_2O) are critical

parameters to consider. Liu *et al.* [39] observed that at a v/m ratio of 9, the gel network remains incompletely formed and undergoes considerable shrinkage. A highly efficient 3-dimensional network structure is achieved at a ratio of 10, yielding a surface area of 809.9 m^2/g and a pore volume of 2.61 cm^3/g. The silica-to-water ratio should be consistently kept within the range of 0.065 - 0.160. An insufficient ratio would hinder the gelation process because of excessive particle spacing, whereas an overly high ratio would lead to instability in the gel structure.

Figure 3 illustrates the sol–gel process via atmospheric pressure drying (APD), encompassing key stages such as gelation, aging, and drying. This process results in the formation of a highly porous silica aerogel structure.

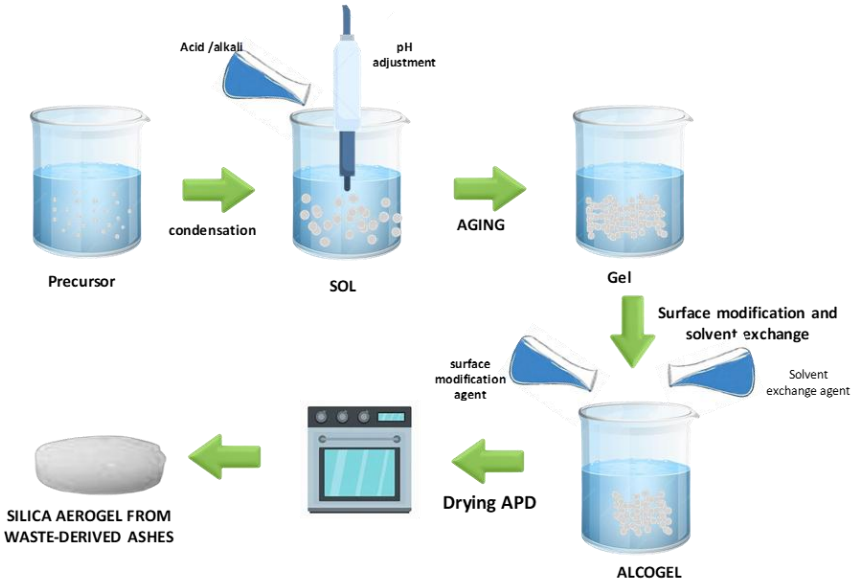

Figure 3 Schematic diagram of sol-gel process via APD drying.

Aging and strengthening process

The duration and temperature of the aging process have a significant impact on the final pore texture of silica aerogels (SA). Research indicates that silica aerogels exhibiting optimal thermal stability and bulk density are typically synthesized via moderate temperature treatment (40 - 50 °C) for a duration of 3 to 24 h [25,31]. Increasing the aging time from 1 to 3 days results in a gradual enhancement of specific surface area, total pore volume, and pore diameter. However, after surpassing the 3-day threshold, these pore properties tend to stabilize, suggesting that the gel system has achieved structural equilibrium [27].

The precursor type significantly influences the required aging duration alongside temperature. FA, characterized by its high amorphous silica content, demonstrates accelerated polycondensation kinetics, which frequently negates the necessity for supplementary aging at ambient temperature (25 °C). Conversely, bottom ash (BA), which exhibits lower silica reactivity, necessitates an aging period of up to 24 h to attain comparable network stability [34]. Furthermore, the selection of the aging medium yields differing results; water treatment results in a more interconnected network with a surface area of 633.39 m2/g and a pore diameter of 3.72 nm, whereas hexane leads to a reduced surface area of 560.87 m^2/g and a broader pore size distribution [35].

Aging markedly affects the production of waste-derived SA by modulating network transformation and improving gel resistance to capillary pressures during APD. This process is governed by continuous polycondensation, which enhances the density of Si–O–Si linkages and cross-linking sites until the gel attains an equilibrium state. Strengthening the gel is essential to ensure that the pore structure can withstand internal pressure and avoid structural collapse during solvent evaporation, thereby creating a more rigid framework [31,40]. Xie *et al.* [37] highlight that aging contributes

nearly 5 times more to the final quality of aerogels than the precursor ratio used during the initial sol-gel phase.

The acceleration of network maturation can occur without significant volumetric shrinkage or internal stress by utilizing an optimal temperature range of 40 - 50 °C. This suggests that regulating aging temperature is a more effective and cost-efficient method for enhancing aerogel quality than focusing exclusively on sol-gel ratio optimization. The efficacy of water as a medium, compared to hexane, is attributed to its uniformity and ability to facilitate accelerated silicate condensation. In contrast, non-polar solvents like hexane inhibit the diffusion of catalysts into the aqueous phase, consequently decreasing the condensation rate and restricting the development of the 3-dimensional network's full potential.

Solvent exchange and surface modification

Surface modification is a critical stage in the synthesis of SA derived from FA and biomass ash, particularly when employing atmospheric pressure drying (APD). In broader nanocomposite systems, moisture sensitivity and non-uniform nanoparticle dispersion have been identified as key factors contributing to structural instability and performance degradation under environmental exposure [41,42]. Excessive filler loading may induce agglomeration and compromise mechanical integrity, underscoring the importance of interfacial control in stabilizing nanostructured architectures. These observations reinforce the necessity of effective surface and interfacial engineering strategies when designing mechanically robust porous materials [41]. Silica gels rich in silanol (Si–OH) groups are highly susceptible to pore collapse during solvent evaporation due to intense capillary forces. The substitution of these polar Si–OH groups with hydrophobic methyl groups (–CH_3) is an effective strategy to reduce capillary tension and preserve the integrity of the aerogel's mesostructured [40,43].

Prior to modification, pore water is displaced by organic solvents with lower surface tension through a methodical solvent exchange process. Ethanol and hexane are commonly utilized to enhance system compatibility for the silylation reaction, enabling a more homogeneous conversion of Si–OH to Si–CH_3 [8]. Without adequate exchange, silylation efficiency drops drastically, leading to denser microstructures with limited mesoporosity [43,44]. Alif *et al.* [44] stated that increasing the solvent exchange duration from 3 to 9 days facilitates a clear transition from xerogel to high-quality SA. The 9-day period yielded SA with the lowest density (0.048 g/cm³), the highest aerogel volume fraction, a BET surface area of 668.82 m²/g, and an average pore size of 25 nm. Similar trends were reported in independent studies using comparable solvents, suggesting reproducible behavior across a wide range of waste-derived silica sources.

During silylation, silane sources such as trimethylchlorosilane (TMCS) react with pore water, ethanol, and silanol groups to form hydrophobic surfaces. The ethanol-hexane mixture is often preferred because ethanol slows down the TMCS reaction kinetics, while hexane effectively displaces pore water and minimizes capillary effects [43,44]. However, the dosage of silane must be carefully managed. Tessema *et al.* [45] observed that excessive silane relative to the ethanol-hexane ratio can reduce the modified silica gel's surface area. For instance, varying TMCS:ethanol:hexane ratios between 50:25:100 and 25:25:100 resulted in surface areas ranging from 630.732 to 909.250 m²/g, while pore volume remained relatively stable.The choice of silane agent significantly dictates the final textural and chemical properties of the SA. Zhang *et al.* [31] reported that modified SA exhibits increased hydrophobicity but often shows a decrease in specific surface area and an increase in average pore size compared to unmodified samples. The hydrophobic transformation is directly correlated with the replacement of Si–OH groups by $Si(CH_3)_3$ moieties, which can be verified by the appearance of Si–C and C–H stretching bands in FTIR spectra. This substitution reduces hydrogen bonding within the pore walls and suppresses capillary condensation during drying [44].

TMCS modification, for example, can increase pore volume up to 3.29 cm³/g (compared to 0.37 cm³/g in unmodified gel) and enhance the contact angle from 89° to 140° [8]. In comparison, agents like KH-570 and MTMS yield contact angles of 123° and 130°, respectively, though MTMS may lead to a more significant reduction in surface area to approximately 146.8 m²/g [31].

Further investigations by Gao *et al.* [40] comparing DMDC, TMCS, and HMDZ showed that

HMDZ provided the lowest density (0.093 g/cm³), the largest pore volume (2.42 cm³/g), and the highest surface area with the narrowest pore distribution. Similarly, Lei *et al.* [31] utilized hexamethyldisiloxane (HMDSO), achieving SA with a density of 110 mg/cm³ and a contact angle of 116°. Interestingly, the simultaneous use of 2 silane agents, such as TMCS and HMDS, can accelerate silanol substitution but requires precise balancing. Higher TMCS content may trigger excessive network restructuring, causing pores to enlarge (5.7 - 11 nm) and surface area to decrease. Conversely, increased HMDS effectively enhances hydrophobicity by ensuring silanol replacement with methyl groups without significant loss in pore volume [46,47].

Ultimately, successful surface modification is indicated by the exclusion of polar phases from the pore structure and the dominance of hexane as the pore fluid, allowing for ambient pressure drying without significant structural collapse [26]. Transitioning from conventional magnetic stirring to ultrasonic agitation has also demonstrated favorable outcomes by promoting uniform particle dispersion and enhancing textural quality [48].

Several sol-gel and APD-based studies have identified network reinforcement approaches that do not involve silylation as a surface modification technique. Pure silica particles, including tetraethyl orthosilicate (TEOS), enhance the 3D framework and reduce gel shrinkage during the APD process. This is achieved by increasing the degree of cross-linking and the mechanical integrity of the silica framework, resulting in a gel structure with greater resistance to capillary forces, despite its limited hydrophobicity.

Tadjarodi *et al.* [46] demonstrated that the addition of TEOS as a silica source can enhance interparticle bonding. This facilitates reduced volume shrinkage and maintains the mesoporous structure during APD. Furthermore, Akhter *et al.* [49] reported a study in which TEOS-added aerogels exhibited higher dimensional stability and structural integrity, despite the resulting aerogels having lower specific surface areas compared to silylated aerogels. These findings indicate that in the synthesis of sol-gel and APD-based aerogels, surface modification and network reinforcement are 2 distinct but complementary mechanisms. The choice of approach generally depends on the need to balance hydrophobicity, mechanical stability, and final performance of the aerogel in relation to the intended application.

This reinforcement strategy primarily increases cross-link density within the silica backbone, thereby improving elastic recovery during solvent evaporation, although it does not directly reduce surface energy as effectively as methyl substitution. Consequently, reinforcement and hydrophobization should be viewed as complementary but mechanistically distinct approaches in APD optimization.

Atmospheric Pressure Drying (APD)

The textural quality of waste-derived ash SA is notably influenced by the APD stage. Qin *et al.* [8] found that a drying temperature of 90 °C for 24 h resulted in SA with a density of 0.0915 g/cm³, porosity of 95.82%, and a surface area of 510 m²/g. Increasing the temperature to 120 - 150 °C led to a twofold increase in density, along with a significant reduction in surface area and pore volume as a result of network collapse. The structural failure observed at elevated temperatures is initiated by a pronounced evaporation gradient, which enhances capillary forces to levels that exceed the strength of the network.

Mechanistically, the collapse during APD is closely associated with capillary forces generated when a liquid-vapor interface forms inside mesopores; condensation reactions occurring during atmospheric drying can amplify capillary stress and trigger skeleton fragmentation and structural collapse [23]. This risk is exacerbated when the gel surface remains rich in silanol groups (Si–OH), because silanol-terminated networks are prone to irreversible condensation during ambient pressure drying, locking the structure in a densified state [50].

To overcome this internal stress, the success of APD relies heavily on the spring-back effect. Based on the findings of Zemke *et al.* [51], this effect is the ability of the gel network to reversibly shrink during solvent evaporation and then expand (spring back) to its original volume. This mechanism is made possible through surface modification (silylation) that replaces reactive hydroxyl (Si–OH) groups with hydrophobic organic groups. This prevents the formation of permanent siloxane (Si–O–Si) bonds when the network shrinks,

allowing the silica framework to recover after capillary pressure is relieved.

Numerous studies have utilized stepwise drying schemes to alleviate internal stress. Cheng *et al.* [14] employed a temperature range of 60 - 180 °C with 2-hour intervals at each step. In contrast, Liu *et al.* [24] applied 40 °C for 24 h, followed by 120 °C for 2 h, to attain a more stable 3D framework. Mermer and Piskin [34] found that consistent drying at temperatures of 60, 80, 120, and 180 °C did not result in significant performance changes. This indicates that the effectiveness of stepwise drying is largely influenced by the initial gel conditions, particularly the degree of cross-linking and the effectiveness of surface hydrophobization.

This dependence on initial gel conditions is consistent with evidence that network strength prior to drying governs whether the framework can withstand capillary pressure under APD. For example, Feng *et al.* [33] reported that low-modulus water glass yields a loose, poorly cross-linked structure whose strength is insufficient to withstand capillary pressure during ambient pressure drying, whereas higher modulus promotes stronger cross-linking and a more robust 3D network. From this standpoint, stepwise drying primarily helps when the gel network has reached a cross-linking threshold and the surface has been adequately hydrophobized—otherwise, temperature programming alone cannot fully prevent collapse [33].

The drying method significantly influences the final properties. The air dryer method has shown greater effectiveness, achieving a specific surface area of 287.7 m^2/g and a mesoporous volume of 0.923 cm^3/g, exceeding the results of freeze-drying and vacuum oven drying in maintaining the porous structure [38]. Air dryers provide uniform heating and efficient hot air contact, leading to reduced shrinkage. SA generated via the APD method consistently exhibits nanopores in the range of 5 to 12 nm, with total porosity between 80% and 91%.

From a manufacturing standpoint, APD represents the most viable option for large-scale production, owing to its straightforward process and cost efficiency. It provides enhanced industrial readiness by eliminating the requirement for intricate vacuum systems or energy-demanding extreme temperatures. Successful APD necessitates a cohesive integration of drying parameters, solvent exchange, and surface modification. Managing capillary tension during solvent evaporation is a significant challenge; slow evaporation at moderate temperatures (90 °C) enables the silica network to adapt to internal tension without incurring permanent deformation [8,28]. A systematic drying approach is essential for generating waste-derived SA with stable structural and functional properties suitable for commercial use [52]. In practice, APD robustness is maximized when (i) solvent exchange/silylation is implemented before drying and and (ii) gelation/precursor routes yield uniform mesoporous networks, since both factors reduce susceptibility to capillary-stress-driven densification during APD [30].

Table 2 illustrates the relationship between processing parameters, microstructure, and properties of silica aerogels. Each processing stage influences the pore structure and ultimately determines the material performance.

Table 2 Summary of process-microstructure-property correlations for waste-ash-derived silica aerogels produced via sol-gel and atmospheric pressure drying.

Key stage or parameter	Microstructural indicator (structure)	Effect on properties (property)	Practical implication
Increased availability of reactive silica and improved homogeneity of the silicate sol	More uniform gel network and more even pore-size distribution	BET surface area tends to be higher, density tends to be lower, and pore stability is improved	Reduces network heterogeneity and defects that promote pore collapse

Key stage or parameter	Microstructural indicator (structure)	Effect on properties (property)	Practical implication
Adequate aging conditions	Stronger gel skeleton and increased network connectivity	Drying shrinkage is reduced and surface area is better preserved	Lowers the risk of pore collapse under atmospheric pressure drying
Effective solvent exchange	Lower surface tension of pore liquid and reduced diffusion gradients	Shrinkage is reduced and porosity is better maintained	Decreases capillary forces that drive shrinkage and microcracking
Surface modification, silylation)	More hydrophobic surface and lower surface energy	Capillary pressure is reduced, shrinkage is lower, and contact angle is higher	A critical step to preserve nanoporous structure during atmospheric pressure drying
Well-controlled atmospheric pressure drying conditions (appropriate drying rate and temperature program)	Better preservation of pore network with fewer microcracks and reduced pore collapse	Lower density, higher BET surface area, and more stable thermal conductivity due to retained porosity	Controlling the drying rate helps reduce shrinkage caused by capillary stress and makes atmospheric-pressure processing more scalable.

Table 3 Summary of APD-derived waste-based silica aerogels and their textural properties.

No.	Silica source	Key synthesis route*	Surface modification	SSA ($m^2 g^{-1}$)	Density ($g cm^{-3}$)	Key remarks	Ref
1	Oil shale ash	Alkali extraction → ion-exchange gelation → APD	DMDC/TMCS/ HMDZ	800 - 980	0.084 - 0.11	HMDZ provides superior structural stability; ink-bottle pores observed	[40]
2	Fly ash	Alkali extraction → acid vs resin-controlled gelation → APD	TMCS	362 - 908	–	Resin-exchange gelation yields markedly higher SSA	[30]
3	Bagasse ash	Alkali extraction → acid gelation → APD	TMCS/HMDS	450 - 1114	–	Water aging enhances SSA; HMDS gives maximum SSA	[35]
4	Fly ash	Trona-assisted extraction → acid gelation → APD	TMCS	516 - 856	0.05 - 0.20	Trona substitutes NaOH, significantly reducing cost	[26]
5	RHA	Alkali extraction → acid gelation → hybrid sol–gel → APD	TEOS	240 - 312	0.12 - 0.18	TEOS improves mesoporous structural integrity	[49]
6	Coal fly ash	Alkali extraction → acid gelation → APD	TMCS	420 - 510	0.092 - 0.12	Optimal drying temperature minimizes density	[8]
7	Lignite FA	Alkali washing → extraction → acid gelation → APD	TMCS	465 - 810	–	Alkali washing removes impurities and boosts SSA	[25]
8	RHA	Alkali extraction → acid gelation → heat treatment	TMCS	611 - 821	–	Heat treatment tunes surface hydroxyl density	[53]
9	RHA	Alkali extraction → pH-controlled gelation → APD	TMCS	511 - 730	0.071 - 0.124	Optimal gelation at pH ≈ 5	[36]
10	FA acid sludge	Alkali extraction → acid gelation → APD	TMCS	668 - 700	0.085 - 0.691	Surface modification prevents pore collapse	[14]
11	FA acid sludge	Alkali extraction → optimized TMCS modification → APD	TMCS	176 - 830	0.072 - 0.165	TMCS ratio controls density linearly	[43]
12	RHA	Alkali extraction → resin decationization → acid gelation → APD	TMCS	786 - 945	0.07 - 0.11	Extremely low density via modulus control	[33]
13	RHA	Alkali extraction → controlled acid titration → APD	TMCS	385 - 861	0.03 - 0.10	Highly hydrophobic and thermally stable	[54]

No.	Silica source	Key synthesis route*	Surface modification	SSA ($m^2 g^{-1}$)	Density ($g cm^{-3}$)	Key remarks	Ref
14	RHA	Alkali extraction → acetic acid gelation → bead APD	TMCS	669	0.048	Long solvent exchange maximizes SSA	[44]
15	Fly ash	Alkali fusion → acid leaching → sol–gel → APD	TMCS	35	0.12	Dense networks limit SSA despite high yield	[28]
16	Fly ash	Calcination → acid gelation (NH_3-assisted) → APD	MTMS	481 - 810	0.082 - 0.085	Excellent thermal stability for insulation	[24]
17	Coal FA	Alkali/acid leaching → sol–gel → APD	MTMS/KH-570	570	0.183	Silane coupling enhances mechanical strength	[31]
18	Bagasse ash	Alkali extraction → resin purification → base gelation → APD	TMCS/HMDS	450 - 1360	–	Ion-exchange critical for ultrahigh SSA	[50]
19	RHA	Sol–gel bead formation → APD	TMCS	773	0.055	Optimized silylation improves bead stability	[55]
20	FA / BA	Ultrasonic-assisted sol–gel → APD	TMCS	338 - 365	0.09 - 0.12	Lower SSA than TEOS-derived aerogels	[34]
21	Fly ash	Alkali leaching residue → sol–gel → APD	HMDSO	538	0.108 - 0.110	Alkali activation improves desilication	[23]
22	Fly ash	Acid–alkali leaching → sol–gel → APD	KH-570/MTMS	147 - 488	0.183 - 0.184	Surface strengthening lowers density	[31]
23	Wheat husk ash	Alkali extraction → resin purification → base gelation → APD	TMCS	513 - 587	0.056 - 0.158	Excellent thermal insulation performance	[39]
24	Fly ash	Alkali fusion → leaching → sol–gel → aging → APD	–	556 - 661	–	Silica-alumina composite; mesoporous	[27]
25	RHA	Alkali extraction → acid gelation → hybrid APD	TEOS	315	~0.32	TEOS mitigates shrinkage during APD	[46]
26	Coal gangue	Na_2CO_3-assisted calcination → sol–gel → APD	TMCS	494	0.348	Efficient silica recovery from complex waste	[22]
27	CFB fly ash	Alkali sintering → acid gelation → APD	TMCS	400 - 550	0.09 - 0.15	Lower-energy sintering route	[56]
28	RHA	Alkali extraction → acid gelation → APD	TMCS	468 - 564	0.14 - 0.20	Uniform mesoporous structure at low TMCS	[57]

Table 3 presents a comparative summary of waste-derived silica aerogels produced via atmospheric pressure drying (APD), including synthesis routes, surface modification, and their textural properties. This table highlights how variations in synthesis strategies and surface treatments significantly influence the specific surface area and density of the resulting materials.

Applications of silica aerogels from waste-derived ashes

The key to successful optimization of synthesis parameters, from the pre-treatment stage to the drying of APD, lies in the application flexibility of the resulting material. A literature review shows that the current trend in waste-derived ashes-based SA synthesis is shifting toward atmospheric pressure drying (APD) to increase industrial scalability.

Figure 4 illustrates the potential applications of silica aerogels derived from waste-based sources across various fields, including thermal insulation, biomedicine, catalysis, and environmental applications. This figure highlights the versatility of silica aerogels, driven by their unique porous structure and physicochemical properties.

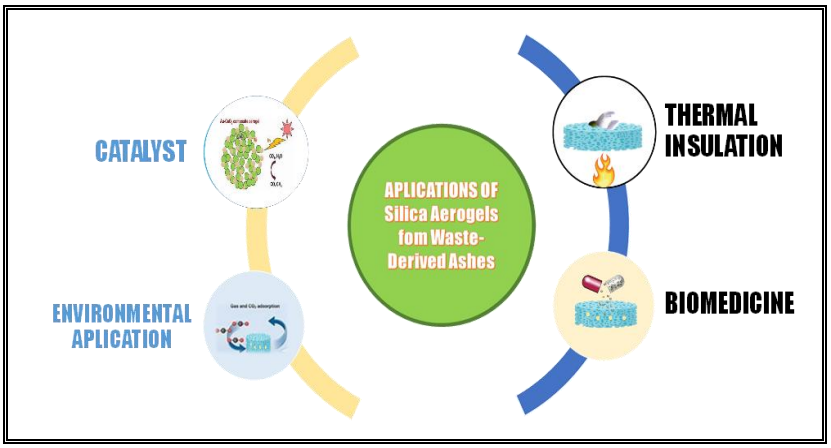

Figure 4 Applications of silica aerogels in various fields.

Thermal insulation

Recent studies on thermal insulators emphasize the use of renewable materials, energy-efficient methods, and waste utilization to reduce dependence on petroleum [58]. Silica Aerogel has emerged as a promising next-generation insulation material in the construction industry such as panels, mortar fillers, and as building additives, due to its exceptional thermal properties [18,54]. Unfortunately, the application of SA in materials is still limited by high production costs and inadequate interfacial bonding between the aerogel and the matrix, which leads to reduced mechanical properties [49].

Li *et al.* [56] revealed that in gypsum-based materials, thermal conductivity decreases with increasing aerogel content. Furthermore, gypsum exhibits adequate fire resistance, characterized by a slowing of the rate of surface temperature rise when exposed to fire. In various construction applications, the addition of SA up to 50% (vol.) to a cement mortar system significantly reduced the thermal conductivity from 1.67 to 0.42 W/m³. However, increasing the SA fraction led to a decrease in mechanical properties; the addition of aerogel particles increased the porous structure of the cement-based composite, thereby reducing its compressive strength. In other words, the addition of high concentrations of SA to the material caused excessive void formation, resulting in a degradation of mechanical properties. Therefore, composition optimization is essential to achieve a balance between thermal performance and structural strength [10].

The mechanical problems of waste aerogels can be addressed using polymer fiber hybridization techniques, as demonstrated in the development of a silica aerogel composite based on rice husk ash and waste plastic fiber (rPET) by Do *et al.* [59]. Through a hybrid structure of 4 layers of rPET fibers alternating with aerogel layers, this material achieved high mechanical stability with a Young's modulus of 84.099 kPa and a load capacity of up to 695 times its own weight. In addition to superior mechanical durability, this integration maintains the typical thermal characteristics of aerogel with low conductivity (0.040 - 0.056 W/m.K) and slow flame propagation speed (0.27 mm/s), making it an innovative solution for energy-efficient and fire-resistant building construction materials.

Separate investigations have shown that LDPE-aerogel composites can reduce thermal conductivity (0.0926 - 0.1820 W/m.K) better than pure LDPE [60]. SA, as an effective additive in paints with low thermal conductivity (0.01 W/m·K), can reduce surface temperatures by up to 5 °C [61]. Furthermore, SA particle size influences the characteristics of polyester resin composites (UPSA). The use of 3 mm granular particles resulted in the most significant reduction in conductivity, reaching 61% (0.1808 W/m²), along with optimal thermal stability. However, this increased material fragility due to the fragile aerogel base structure ([62]. Overall, research on ash-based sol–gel materials for thermal insulation remains largely confined to the laboratory scale, with limited data on long-term durability and performance consistency across heterogeneous waste sources.

Environmental remediation

In addition to their application in construction, the high porosity and adjustable surface characteristics of silica aerogels further motivate their investigation for environmental remediation purposes. The potential of ash-based silica aerogels in addressing environmental issues stems from their adaptive pore architecture and massive specific surface area, which allow for efficient chemical modification. The effectiveness of this material fundamentally depends on a precise interaction between its internal pore architecture and the specific functional groups bonded to the silica surface.

To reduce greenhouse gas emissions, the use of SA, both in pure and amine-modified forms, has proven to be an effective method for carbon dioxide (CO_2) capture [63,64]. This material can achieve an adsorption capacity of up to 880 mmol/g CO_2 under optimal conditions [15,65]. Specifically, the amine-modified variety (AMSA) exhibits a capacity of 52.40 cm^3/g, initiated by a rapid chemical reaction and followed by a physical adsorption process until saturation is reached. AMSA's advantage also lies in its impressive durability, with the material able to survive ten reuse cycles with less than 10% performance degradation [65]. Furthermore, the development of a Lithium Silicate (Li_4SiO_4)-based adsorbent, which is synthesized from fly ash (FA)-based silica aerogel with natural doping of Al, Fe, and Ti, has demonstrated outstanding high-temperature CO_2 capture performance, reaching 33.24 wt% in just 7.0 min [64]. The adsorption capacity of this FA-based material also demonstrated remarkable stability, retaining over 70% of its efficacy after 35 consecutive cycles of use.

In addition to gas capture, ash-derived aerogels have also been documented to effectively facilitate the removal of heavy metal ions from aqueous solutions [66]. Numerous studies have demonstrated high adsorption efficiencies for Pb^{2+} [19,51,76] and U(VI), reaching up to 97.6% [20,68]. According to Yan *et al.*, [68], SiO_2–Al_2O_3 composite aerogels modified with APTES were reported to adsorb 195 mg/g of Cu^{2+} and 500 mg/g of Pb^{2+} within only 10 min.

Beyond heavy metals, SA shows enormous promise in cleaning up food products and pharmaceuticals. Merve *et al.* [36] explain aerogel in sunflower oil processing, demonstrate super-performance compared to the traditional material, bentonite. By TSA achieving a removal of approximately 32.2% of free fatty acids (FFA). The uniform pores of the material function as conduits, facilitating the diffusion of drug pollutants such as amoxicillin and erythromycin into active sites, resulting in removal rates reaching 90% [69].

The description is similar for organic dyes such as methylene blue and Congo red. Heat treatment of the SA at 500 °C results in a closely threefold increase in capacity, more than 420 mg/g for both dyes [53]. The improvement occurs as the heat treatment increases surface area and generates hydroxyl "hooks" that attract dye molecules. Although SA displays inherent water-repellent properties, the process of thermal alteration is crucial for enhancing its dispersion in water, thereby permitting it to address a broader range of industrial dyes effectively [70].

While adsorption-based remediation exploits the large surface area and pore accessibility of ash-derived silica aerogels, these same structural advantages can be further leveraged by incorporating catalytically active species, transforming the aerogel framework from a passive sorbent into an active catalytic platform.

Catalyst support

SA's high-heat stability and high surface area make it a candidate for a biocatalyst support. Several studies have demonstrated the effectiveness of SA as a catalyst support. For example, Wang *et al.* [15] used an SA-Al_2O_3 composite from ash as a support for TiO_2 nanoparticles. The synergy between the adsorption capacity of the aerogel framework and the photocatalytic activity of TiO_2 successfully degraded the organic pollutant di-n-butyl phthalate (DNBP) under visible light irradiation without a significant decrease in efficiency after 5 reuse cycles [15].The application of silica alumina aerogel obtained from rice husk ash for the immobilization of iron oxide nanoparticles (γ-Fe_2O_3) demonstrated its efficacy in degrading Rhodamine B via a photo-Fenton-like process [16]. The synthesis of Fe_3O_4@TiO_2 core-shell microspheres using fly ash silica has improved operational efficiency, facilitating rapid magnetic separation at ambient temperature. The Fe_3O_4@TiO_2/SiO_2 magnetic composite exhibited significant efficacy in degrading Rhodamine B, maintaining consistent performance after 6 cycles of repeated use [71].

Beyond environmental and catalytic functions, the exceptional porosity, high surface area, and structural tunability of waste-derived silica aerogels have also attracted growing interest in biomedical applications, where controlled mass transport and surface interactions are critical.

Biomedical applications

The study of waste-derived SA in the biomedical field is a very promising research area, particularly related to drug delivery systems and tissue engineering. SA's high porosity and considerable specific surface area enable it to contain a large number of hydrophobic medicinal molecules [18]. This material had a loading capacity of 0.87 g of ibuprofen per gram of SA, with a quick initial release followed by a progressive and regulated release [17]. Solid adsorbents based on RHA, constructed as hollow microspheres, enhanced the dissolving rate of weakly water-soluble medicines, thereby enhancing pharmaceutical bioavailability [72].

In addition to functioning as drug carriers, waste-derived SA exhibited significant bioactive properties that are beneficial for bone tissue engineering. This material retained its porous structure after calcination and promoted the formation of an apatite layer when interacting with Simulated Body Fluid (SBF) solution [73]. However, the effectiveness of this bioactivity is highly dependent on accurate compositional regulation; increasing silica concentration has been shown to inhibit bone mineralization. Investigation of the Hydroxyapatite-Silica Aerogel (HAESA) system revealed that the material's biocompatibility is largely influenced by the HA/SiO_2 ratio. Silica-rich ash increased fibroblast cell viability and proliferation by up to 180% after 48 h [74].

The integration of hydroxyapatite within the silica network at an optimal ratio improves structural and biological properties, offers mechanical support, and creates a conducive environment for soft and hard tissue growth. Although studied *in vitro*, waste-based SA shows significant potential as a biomaterial that integrates the circular economy with advanced healthcare technologies.

Research gap and future outlook

Research gaps

Although the current literature provides a strong foundation for waste-based silica aerogel synthesis, this systematic review reveals several research gaps that hinder the technology's transition from laboratory scale to commercial applications.

Waste precursor standardization and dominance of ash sources

Currently, the dominant use of coal ash and rice husks is not accompanied by strict precursor standardization protocols. The variability in the chemical composition of these two primary sources often results in inconsistencies in the textural quality of the final aerogel. Therefore, a standardization framework is needed to bridge the differences in waste profiles and ensure the stability of the mesoporous structure during the sol-gel process, which culminates in ambient pressure drying (APD). Based on a literature review, fly ash, particularly from coal combustion and rice husk biomass ash, dominates as a precursor source for silica aerogels. Exploration of other alternative ash sources remains very limited. This situation creates a knowledge gap regarding silica extraction methods for various waste chemical characteristics, thus broadening the raw material base for the aerogel industry in the future.

Temporal efficiency and process kinetic optimization

The long SA synthesis time, particularly during the aging, solvent exchange, and APD drying stages, is a major obstacle in the transition from laboratory scale to mass production. The long SA synthesis time emphasizes the need for process intensification to increase throughput. However, to date, no research has explored the use of accelerating catalysts or rapid diffusion techniques that can reduce process time without compromising the integrity of the pore structure. Therefore, time efficiency is often overlooked. This aspect is often neglected in the sustainability analysis of aerogel synthesis processes that use waste ash.

Mechanical-thermal balance and interfacial integration at large scale

Current literature over-relies on textural parameters, such as surface area and pore volume, while mechanical aspects are often neglected. The interfacial bond between SA and the composite matrix (such as cement or gypsum) appears weak, leading to brittleness, as the chemical strengthening mechanisms at the molecular level to prevent structural failure have not been thoroughly explored.

Future outlook

The development of waste ash-based silica aerogel has shown promising results. However, the transition to industrial applications still requires a strategic roadmap. In the future, SA synthesis research should prioritize the following:

Standardization of protocols and diversification of silica sources

Standardization of protocols and diversification of silica sources. SA synthesis research must establish standard raw material parameters. This standardization aims to mitigate the chemical variability of various types of waste ash. Furthermore, this method can be extended to alternative raw materials besides coal combustion ash and rice husk ash, such as palm oil ash (POFA), sawdust, and municipal waste incineration ash. However, these sources require strict purification protocols and leaching methods to eliminate heavy metal contaminants. A successful transition will ensure the functional stability of silica aerogel. Ultimately, this material can be commercially and sustainably applied.

Acceleration of process kinetics and temporal efficiency

Future research is expected to focus on reducing process time. The aging and solvent exchange stages are time-consuming, sometimes even days. Reducing production time will undoubtedly increase economic competitiveness. This factor is a key determinant of the position of silica aerogel from ash in the global market. Innovation can be achieved through the application of microwave-assisted, ultrasonic-assisted, or continuous flow technologies.

Application-oriented engineering

Future silica aerogel design will evolve toward interface engineering at the molecular level, such as the use of coupling agents to ensure strong and stable bonds between the aerogel and the supporting matrix. This approach is applied to cement- or gypsum-based construction materials, given their massive usage volume and the demands for mechanical performance and long-term durability.

Techno-economic integration

The future focus is on filling research gaps by integrating synthesis parameters with energy consumption, production costs, and environmental impact analysis (Life-cycle Assessment). This includes a transition to Green Chemistry, such as replacing toxic organic solvents with green solvents, to strengthen the position of waste-based silica aerogel as a sustainable material.

Conclusions

A literature review (SLR) shows that silica aerogel (SA) can be effectively synthesized from waste ash precursors through a sol-gel process combined with atmospheric pressure drying (APD). Gel network formation is strongly influenced by sol-gel parameters, including the type of acid, sol pH, acid-to-ash ratio, and silica-to-water ratio. These parameters collectively determine the hydrolysis–condensation kinetics and pore development. Strict control of these factors is necessary to produce a homogeneous mesoporous network with a high surface area. The Deviations from optimal conditions can lead to overcrowding or unstable colloidal structures.

APD offers more simple and more economical, but its effectiveness is highly dependent on the sol chemistry and surface modification techniques to minimize pore shrinkage and collapse. Most studies have focused on the specific surface area, total pore volume, average pore size, density, and hydrophobicity of the resulting aerogels. The utilization of waste ash-based silica aerogel for practical applications requires an integrated strategy that links synthesis optimization, process management, and property-performance evaluation, so that laboratory findings can be applied on a large scale and sustainably.

Acknowledgements

The authors would like to express their sincere gratitude to the Indonesian Education Scholarship (Beasiswa Pendidikan Indonesia), the Center for Higher Education Funding and Assessment, Ministry of Higher Education, Science, and Technology of the Republic of Indonesia, and the Endowment Fund for Education Agency (Lembaga Pengelola Dana Pendidikan), Ministry of Finance of the Republic of Indonesia, for their support under decree number NO. 02953/J5.2.3./BPI.06/10/2022 and BPI ID: 202231103519.

Declaration of Generative AI in Scientific Writing

During the preparation of this work, the author(s) used Gemini AI in order to improve the language and readability of the manuscript. After using this tool, the author(s) reviewed and edited the content as needed and take(s) full responsibility for the content of the published article.

CRediT Author Statement

Iwan Rusiardy: Collected and analyzed the data. **Sukma Surya Kusumah:** Conducted the investigation and prepared the original draft. **Muhammad Romli:** Development methodology and supervised the study. **Erliza Noor and Suprihatin:** Reviewed and edited the manuscript.

References

[1] A Lamy-Mendes, ADR Pontinha, P Alves, P Santos and L Durães. Progress *in silica* aerogel-containing materials for buildings' thermal insulation. *Construction and Building Materials* 2021; **286**, 122815.

[2] KM Omatolaa, AD Onojah, AN Amah and I Ahemen. Synthesis and characterization of silica xerogel and aerogel from rice husk ash and pulverized beach sand via sol-gel route. *Journal of the Nigerian Society of Physical Sciences* 2023; **5**, 11609.

[3] NS Indrasti, A Ismayana, A Maddu and SS Utomo. Synthesis of nano-silica from boiler ash in the sugar cane industry using the precipitation method. *International Journal of Technology* 2020; **11(2)**, 422-435.

[4] ZT Yao, XS Ji, PK Sarker, JH Tang, LQ Ge, MS Xia and YQ Xi. A comprehensive review on the applications of coal fly ash. *Earth-Science Reviews* 2015; **141**, 105-121.

[5] JI Odzijewicz, E Wołejko, U Wydro, M Wasil and A Jabłońska-Trypuć. Utilization of ashes from biomass combustion. *Energies* 2022; **15(24)**, 9653.

[6] H Shen, B Liu, B Lou, J Zhang, X Zhang, H Shen, J Liu and S Zhang. Separation of heavy metals from municipal solid waste incineration fly ash: A review. *Ecotoxicology and Environmental Safety* 2025; **299**, 118363.

[7] AP Wardanu, NS Indrasti and Suprihatin. Green synthesis of silica nanoparticles (Si-NPs) from palm oil fuel ash (POFA) and its application to purification water: A review. *IOP Conference Series: Earth and Environmental Science* 2024; **1358(1)**, 012015.

[8] XH Qin, J Xu, Y Feng, A Tahmasebi and JL Yu. An experimental study on production of silica aero-gel using fly ash from coal-fired power plants. *Advanced Materials Research* 2014; **1010**, 943-946.

[9] L Fan, Y Mu, J Feng, F Cheng, M Zhang and M Guo. In-situ Fe/Ti doped amine-grafted silica aerogel from fly ash for efficient CO_2 capture: Facile synthesis and super adsorption performance. *Chemical Engineering Journal* 2023; **452**, 138945.

[10] C Panyo, A Wannagon, Y Chimupala, JT Pearce and A Nuntiya. Silica aerogel from sugarcane bagasse ash incorporated cementitious thermal insulation composites. *Materials Letters* 2023; **350**, 134903.

[11] AB Rashid, SI Shishir, MA Mahfuz, MT Hossain and ME Hoque. Silica aerogel: Synthesis, characterization, applications, and recent advancements. *Particle & Particle Systems Characterization* 2023; **40(6)**, 2200186.

[12] P Terzioglu, TM Temel, BK İkizler and S Yucel. Preparation of nanoporous silica aerogel from wheat husk ash by ambient pressure drying process for the adsorptive removal of lead from aqueous solution. *Journal of Bioprocessing & Biotechniques* 2018; **8(1)**, 1000315.

[13] S Huang, C Chen, Z Zhao, L Jia and Y Zhang. Highly efficient separation of uranium from wastewater by in situ synthesized hydroxyapatite modified coal fly ash composite aerogel. *Journal of Industrial and Engineering Chemistry* 2023; **118**, 418-431.

[14] Y Cheng, N Li and C Wei. Effect of the TMCS/hydrogel volume ratio on physical properties of silica aerogels based on fly ash acid sludge. *Journal of Sol-Gel Science and Technology* 2016; **78(2)**, 279-284.

[15] HL Wang, HP Qi, XN Wei, XY Liu and WF Jiang. Photocatalytic activity of TiO2 supported SiO_2-Al_2O_3 aerogels prepared from industrial fly ash. *Chinese Journal of Catalysis* 2016; **37(11)**, 2025-2033.

[16] LDORB Fenton. γ-Fe_2O_3 nanoparticles immobilized in SiO_2 aerogel synthesized from rice husk ash for photo. *Green Chemistry* 2018; **11(2)**, 544-553.

[17] SK Rajanna, D Kumar, M Vinjamur and M Mukhopadhyay. Silica aerogel microparticles from rice husk ash for drug delivery. *Industrial & Engineering Chemistry Research* 2015; **54(3)**, 949-956.

[18] Z Ulker and C Erkey. A novel hybrid material: An inorganic silica aerogel core encapsulated with a tunable organic alginate aerogel layer. *RSC Advances* 2014; **4(107)**, 62362-62366.

[19] Ö Başgöz and Ö Güler. The unusually formation of porous silica nano-stalactite structure by high temperature heat treatment of SiO_2 aerogel synthesized from rice hull. *Ceramics International* 2020; **46(1)**, 370-380.

[20] RT Jayanti. Ekstraksi silika dari fly ash pabrik kelapa sawit menggunakan variasi pelarut karbonat (*in Indonesian*). *Jurnal Teknik Kimia USU* 2023; **12(1)**, 9-17.

[21] SK Rajanna, M Vinjamur and M Mukhopadhyay. Mechanism for formation of hollow and granular silica aerogel microspheres from rice husk ash for drug delivery. *Journal of Non-Crystalline Solids* 2015; **429**, 226-231.

[22] J Zhu, S Guo and X Li. Facile preparation of a SiO_2-Al_2O_3 aerogel using coal gangue as a raw material via an ambient pressure drying method and its application in organic solvent adsorption. *RSC Advances* 2015; **5(125)**, 103656-103661.

[23] Z Lei, W Hengliang, L Zhang, J Yang, L Jianwei and W Jingli. A study on preparation and properties of fly ash-based SiO_2 aerogel material. *Colloids and Surfaces A: Physicochemical and Engineering Aspects* 2024; **684**, 133016.

[24] Z Liu, C Zang, S Zhang, Y Zhang, Z Yuan, H Li and J Jiang. Atmospheric drying preparation and microstructure characterization of fly ash aerogel thermal insulation material with superhydrophobic. *Construction and Building Materials* 2021; **303**, 124425.

[25] E Bedir, S Çitoğlu and H Duran. Transformation of fly ash-based oxide particles into a functional silica-alumina aerogel and its potential application as an anti-icing surface. *ACS Omega* 2024; **9(33)**, 35864-35872.

[26] X Wu, M Fan, JF Mclaughlin, X Shen and G Tan. A novel low-cost method of silica aerogel fabrication using fly ash and trona ore with ambient pressure drying technique. *Powder Technology* 2018; **323**, 310-322.

[27] K Sun, Y Liu, Z Zhang, J Xu, J Yu, J Zhang, L Gui, Z Chen and S Liang. Fly ash-derived mesoporous silica–alumina aerogel via an optimized water-acid leaching process for effective methylene blue removal. *Separations* 2025; **12(9)**, 1-16.

[28] J Xia, B Zhao, Y Guo, K Li, Q Na, S He and J Zhang. Synergistic alkali fusion-acid leaching strategy for silica aerogel synthesis from fly ash and performance optimization. *Scientific Reports* 2025; **15(1)**, 40299.

[29] M Criado, M Vicent and FJ García-Ten. Reactivation of alkali-activated materials made up of fly ashes from a coal power plant. *Cleaner Materials* 2022; **3**, 100043.

[30] F Shi, JX Liu, K Song and ZY Wang. Cost-effective synthesis of silica aerogels from fly ash via ambient pressure drying. *Journal of Non-Crystalline Solids* 2010; **356(43)**, 2241-2246.

[31] L Zhang, Q Wang, H Zhao, R Song, Y Chen, C Liu and Z Han. Synthesis and surface strengthening modification of silica aerogel from fly ash. *Materials* 2024; **17(7)**, 1614.

[32] D Dhaneswara, JF Fatriansyah, FW Situmorang and AN Haqoh. Synthesis of amorphous silica from rice husk ash: Comparing HCl and CH_3COOH acidification methods and various alkaline concentrations. *International Journal of Technology* 2020; **11(1)**, 200-208.

[33] Q Feng, K Chen, D Ma, H Lin, Z Liu, S Qin and Y Luo. Synthesis of high specific surface area silica aerogel from rice husk ash via ambient pressure drying. *Colloids and Surfaces A: Physicochemical and Engineering Aspects* 2018; **539**, 399-406.

[34] N Karamahmut Mermer and S Piskin. Silica based aerogel synthesis from fly ash and bottom ash: The effect of synthesis parameters on the structure. *Main Group Chemistry* 2018; **17(1)**, 63-77.

[35] N Nazriati, H Setyawan, S Affandi, M Yuwana and S Winardi. Using bagasse ash as a silica source when preparing silica aerogels via ambient pressure drying. *Journal of Non-Crystalline Solids* 2014; **400**, 6-11.

[36] S Cui, SW Yu, BL Lin, XD Shen and D Gu. Preparation of SiO_2 aerogel from rice husk ash. *RSC Advances* 2015; **5(81)**, 65818-65826.

[37] P Xie, L Zhang, K Jia, G Ma, JC Hower, C Huang and K Liu. Key factors responsible for environment-friendly aerogel fabrication using fly ash: Superior comprehensive performances and mechanism elaboration. *Journal of Non-Crystalline Solids* 2025; **669**, 123827.

[38] TM Temel, BK İkizler, P Terzioğlu, S Yücel and YB Elalmış. The effect of process variables on the properties of nanoporous silica aerogels: An approach to prepare silica aerogels from biosilica. *Journal of Sol-Gel Science and Technology* 2017; **84(1)**, 51-59.

[39] SW Liu, Q Wei, SP Cui, ZR Nie, MH Du and QY Li. Hydrophobic silica aerogel derived from wheat husk ash by ambient pressure drying. *Journal of Sol-Gel Science and Technology* 2016; **78(1)**, 60-67.

[40] GM Gao, XC Xu, HF Zou, GJ Ji and SC Gan. Microstructural and physical properties of silica aerogels based on oil shale ash. *Powder Technology* 2010; **202(1-3)**, 137-142.

[41] AN Hadi, MH Meteab and MK Mohammed. Influence of Inclusion Sb_2O_3/NiO nanostructures on the morphological, microstructural, and optical characteristics of PVA polymeric for gamma-ray shielding applications. *Revue des Composites et des Matériaux Avancés* 2025; **35(3)**, 581.

[42] KK Kadhim, HM Azeez, RT Yousif, MK Mohammed and MH Meteab. Boosting the structural, optical and AC electrical characteristics of PVA/CdTe nanocomposites for flexible smart optoelectronic devices. *International Journal of Nanoelectronics and Materials* 2025; **18(4)**, 527-536.

[43] Y Cheng, M Xia, F Luo, N Li, C Guo and C Wei. Effect of surface modification on physical properties of silica aerogels derived from fly ash acid sludge. *Colloids and Surfaces A: Physicochemical and Engineering Aspects* 2016; **490**, 200-206.

[44] ZAA Halim, MAM Yajid and H Hamdan. Effects of solvent exchange period and heat treatment on physical and chemical properties of rice husk derived silica aerogels. *Silicon* 2021; **13(1)**, 251-257.

[45] B Tessema, G Gonfa, SM Hailegiorgis and SV Prabhu. Synthesis and characterization of modified silica gel from teff straw ash using sol-gel method. *Next Materials* 2024; **3**, 100146.

[46] A Tadjarodi, M Haghverdi and V Mohammadi. Preparation and characterization of nano-porous silica aerogel from rice husk ash by drying at atmospheric pressure. *Materials Research Bulletin* 2012; **47(9)**, 2584-2589.

[47] MYJ Liu, UJ Alengaram, M Santhanam, MZ Jumaat and KH Mo. Microstructural investigations of palm oil fuel ash and fly ash based binders in lightweight aggregate foamed geopolymer concrete. *Construction and Building Materials* 2016; **120**, 112-122.

[48] W Rahayu, S Muthomimah, S Sumari and N Nazriati. Effect of sonication time on characteristics of synthesized silica aerogel activated carbon nanocomposite based on bagasse ash. *IOP Conference Series: Materials Science and Engineering* 2020; **833(1)**, 012088.

[49] F Akhter, DSA Soomro, AR Jamali and VJ Inglezakis. Structural, morphological and physiochemical analysis of $SiC_8H_{20}O_4/C_2H_5O/C_7H_{16}$ modified mesoporous

silica aerogels. *Physical Chemistry Research* 2023; **11(1)**, 1-8.

[50] NH Setyawan and S Winardi. Synthesis of silica aerogel from bagasse ash by ambient pressure drying. *AIP Conference Proceedings* 2011; **1415(1)**, 114-116.

[51] F Zemke, J Gonthier, E Scoppola, U Simon, MF Bekheet, W Wagermaier and A Gurlo. Origin of the springback effect in ambient-pressure-dried silica aerogels: the effect of surface silylation. *Gels* 2023; **9(2)**, 160.

[52] S Shenqiang, M Di Luigi and L An. Scalable and robust silica aerogel materials from ambient pressure drying. *Materials Advances* 2022; **3(3)**, 2726-2736.

[53] CK Chen, Q Feng, D Ma and X Huang. Hydroxyl modification of silica aerogel: an effective adsorbent for cationic and anionic dyes. *Colloids and Surfaces A: Physicochemical and Engineering Aspects* 2021; **616**, 126331.

[54] G Ban, S Song, HW Lee and HT Kim. Effect of acidity levels and feed rate on the porosity of aerogel extracted from rice husk under ambient pressure. *Nanomaterials* 2019; **9(2)**, 300.

[55] Z Alif, A Halim, M Azizi, M Yajid and H Hamdan. Synthesis and characterization of rice husk ash derived - silica aerogel beads prepared by ambient pressure drying. *Key Engineering Materials* 2016; **694**, 106-110.

[56] JY Li, BH Tian, XX Li, Z Wang, LP Cui, DD Liang, SL Wang, YH Liu, HA Ou and HX Liang. Energy effective utilization of circulating fluidized bed fly ash to prepare silicon-aluminum composite aerogel and gypsum. *Waste Management* 2023; **172**, 162-170.

[57] NF Mohamad, NH Abdul Rani, OS Jehan Elham, SH Anaziah Muhamad, SA Muda, Y Basear and MK Mohammed Faisal. Synthesis and characterization of silica aerogel from rice husk with ambient pressure drying method. *Journal of Physics: Conference Series* 2020; **1535(1)**, 012049.

[58] S Silviana, AN Sa'adah, RP Deastuti, NC Ramadhani, N Simarmata, LE Arianto, MY Tiurma, J Rahmaningrum, F Fauzi and MAS Mahmud. Synthesis of silica-cellulose aerogel derived from bagasse through impregnation and ambient pressure drying methods as thermal insulator. *IOP Conference Series: Earth and Environmental Science* 2022; **963(1)**, 012027.

[59] NHN Do, NNT Can and PK Le. Thermal insulation of flame retardant silica aerogel composites from rice husk ash and plastic waste fibers. *Journal of Inorganic and Organometallic Polymers and Materials* 2024; **34(2)**, 522-532.

[60] AH Zulkipli and AZ Romli. Thermal characterization of low density polyethylene (LDPE)/rice husk ash and rice husk ash derived silica aerogel composites. *AIP Conference Proceedings* 2018; **1985(1)**, 030011.

[61] AL Yanru, HD Utomo, YX Jiang and L Xiaodong. Development of water-based thermal insulation paints using silica aerogel. *Journal Name Pending* 2020; **14(5)**, 2020.

[62] ZA Abdul Halim, MA Mat Yajid, MH Idris and H Hamdan. Effects of silica aerogel particle sizes on the thermal-mechanical properties of silica aerogel–unsaturated polyester composites. *Plastics, Rubber and Composites* 2017; **46(4)**, 184-192.

[63] NH Rani, NF Mohammad, SI Jamaludin, NF Teo, NS Sah and MJ Jalil. Synthesis and characterization of amine impregnated silica aerogel from rice husk for CO_2 adsorption. *Recent Innovations in Chemical Engineering* 2020; **13(5)**, 407-417.

[64] Y Mu, T Wang, M Zhang and M Guo. CO_2 high-temperature sorbent (Al, Fe, Ti) CO-doped Li_4SiO_4 from fly ash-derived SiO_2 aerogel: *In-situ* synthesis, enhanced capture ability and long cycle stability. *Fuel Processing Technology* 2023; **239**, 107533.

[65] S Cui, S Yu, B Lin, X Shen, X Zhang and D Gu. Preparation of amine-modified SiO_2 aerogel from rice husk ash for CO_2 adsorption. *Journal of Porous Materials* 2017; **24(2)**, 455-461.

[66] CY Hidayatulloh, AS Iskandar, S Al-ayubi, AR Permanasari and K Kunci. Literature review of the utilization of rice husk silica as an adsorbent aerogel to reduce metal content in water. *Industrial Research Workshop and National Seminar* 2021; **xx(xx)**, 779-784.

[67] VG Le. Ultrahigh Pb^{2+} ion adsorption by EDTA-modified super-porous silica aerogel derived from

rice husk ash. *Environmental Research* 2025; **286(1)**, 122803.

[68] F Yan, Y Liu, H Wang, M Zhang and M Guo. Amino-terminated SiO2–Al2O3 composite aerogels from fly ash for improved removal of Cu^{2+} and Pb^{2+} ions in wastewater: one-pot synthesis, excellent adsorption capacity and mechanism. *Environmental Science and Pollution Research* 2023; **30(9)**, 23655-23667.

[69] YH Ochoa-Munoz, RS Guerrero-Calderón, RM de Gutiérrez and JA Torres-Leon. Rice husk-derived silica aerogels for efficient removal of amoxicillin and erythromycin from water. *Surfaces and Interfaces* 2025; **78**, 108089.

[70] Nazriati, L Maknun and F Fajaroh. Removal methylene blue from aqueous solution using silica aerogel prepared from bagasse ash. *IOP Conference Series: Earth and Environmental Science* 2019; **299(1)**, 012044.

[71] ZD Li, HL Wang, XN Wei, XY Liu, YF Yang and WF Jiang. Preparation and photocatalytic performance of magnetic Fe_3O_4@ TiO_2 core-shell microspheres supported by silica aerogels from industrial fly ash. *Journal of Alloys and Compounds* 2016; **659**, 240-247.

[72] SK Rajanna, M Vinjamur and M Mukhopadhyay. Robust silica aerogel microspheres from rice husk ash to enhance the dissolution rate of poorly water-soluble drugs robust silica aerogel microspheres from rice husk ash to enhance the dissolution rate of poorly water-soluble drugs. *Chemical Engineering Communications* 2017; **204(2)**, 249-253.

[73] NS Sani, NANN Malek, K Jemon, MRA Kadir and H Hamdan. Effect of mass concentration on bioactivity and cell viability of calcined silica aerogel synthesized from rice husk ash as silica source. *Journal of Sol-Gel Science and Technology* 2017; **82(1)**, 120-132.

[74] NS Sani, NANN Malek, K Jemon, MRA Kadir and H Hamdan. Preparation and characterization of hydroxyapatite incorporated silica aerogel and its effect on normal human dermal fibroblast cells. *Journal of Sol-Gel Science and Technology* 2019; **90(2)**, 422-433.